Excitonic singlet-triplet ratio in a semiconducting organic thin film

M. A. Baldo and D. F. O'Brien*
Center for Photonics and Optoelectronic Materials (POEM), Department of Electrical Engineering and the Princeton Materials Institute, Princeton University, Princeton, New Jersey 08544

M. E. Thompson
Department of Chemistry, University of Southern California, Los Angeles, California 90089

S. R. Forrest
Center for Photonics and Optoelectronic Materials (POEM), Department of Electrical Engineering and the Princeton Materials Institute, Princeton University, Princeton, New Jersey 08544

(Received 1 June 1999)

A technique is presented to determine the spin statistics of excitons formed by electrical injection in a semiconducting organic thin film. With the aid of selective addition of luminescent dyes, we generate either fluorescence or phosphorescence from the archetype organic host material aluminum tris (8-hydroxyquinoline) (Alq_3). Spin statistics are calculated from the ratio of fluorescence to phosphorescence in the films under electrical excitation. After accounting for varying photoluminescent efficiencies, we find a singlet fraction of excitons in Alq_3 of $(22\pm3)\%$. [S0163-1829(99)08743-3]

I. INTRODUCTION

An assumption often employed in the study of electroluminescence (EL) in organic materials is that excitons are formed in the ratio of one singlet to three triplets.[1] However, it is not obvious that this should be the case, especially given that exchange interactions reduce the triplet state energy relative to that of the singlet. Accurate knowledge of spin statistics might therefore provide insight into the poorly understood process of exciton formation by electrical injection in conductive organic materials. Furthermore, since only singlets fluoresce, the singlet fraction (χ_s) is required to calculate the efficiency limit for an increasing diversity of fluorescent organic EL materials.[2]

Triplet excitons can be extracted from a semiconducting host material using a phosphorescent dye dopant.[3–6] Since it is well known that singlets can be similarly extracted using a fluorescent dye,[7] it follows that χ_s within a host can be determined if efficient energy transfer is possible to both fluorescent and phosphorescent dyes. In this work, we measure χ_s of the archetype host material, aluminum tris (8-hydroxyquinoline) (Alq_3) under electrical injection by doping it with either the phosphorescent dye, 2,3,7,8,12,13,17,18-octaethyl-21*H*,23*H*-porphine platinum (II) (PtOEP)[3], or the fluorescent dye[7] [2-methyl-6-[2-(2,3,6,7-tetrahydro-1*H*,5*H*-benzo[*ij*]quinolizin-9-*yl*)ethenyl]-4*H*-pyran-4-ylidene] propane-dinitrile (DCM2). We chose Alq_3 as the host material since emission by this compound arises from ligand-localized fluorescence[8] (i.e., no triplet emission). Thus undoped Alq_3 devices provide a second, independent, measurement of the singlet fraction without the complication of energy transfer. Furthermore, Alq_3 is an important organic semiconductor commonly used in organic light emitting devices.[9]

II. THEORY

In guest-host systems such as PtOEP or DCM2 doped into Alq_3, excitons formed in the host are transferred to the luminescent dye via a combination of Förster and Dexter energy transfer.[10] Förster transfer is a long range (~40–100 Å), nonradiative, dipole-dipole coupling of donor (*D*) and acceptor (*A*) molecules. Since it requires that the transitions from the ground to the excited states be allowed for both *D* and *A* species, this mechanism only transfers energy to the singlet state of the acceptor molecule. Dexter transfer is a short-range process where excitons diffuse from *D* to *A* sites via intermolecular electron exchange. In contrast to Förster transfer, Dexter processes require only that the total spin of the *D*-*A* pair be conserved under the Wigner-Witmer selection rules.[10] Consequently, Dexter transfer permits both singlet-singlet and triplet-triplet transfers. Singlet-triplet and triplet-singlet transfers are also possible if the donor exciton breaks up and reforms on the acceptor via incoherent electron exchange.[10] This latter process is considered to be relatively unlikely as it requires the dissociation of the donor exciton, which in most molecular systems has a binding energy of ~1 eV.

Figure 1 summarizes the energy-transfer pathways responsible for guest fluorescence and phosphorescence in a semiconducting host. In Fig. 1(a), we show the singlet-to-singlet transfer responsible for fluorescence in most doped organic EL devices. Although both Förster and Dexter processes are capable of singlet-to-singlet energy transfer, Förster transfer dominates[11] at low fluorescent dye concentrations because of its long-range nature. Indeed, we find that >99% of the photoluminescent (PL) spectra of DCM2:Alq_3 films under modest optical pump intensities ($\lesssim 1$ mW/cm^2) is due to emission only from DCM2. Thus the energy-transfer rate is much faster than either the radiative or nonradiative rates in Alq_3. Significantly, this means that singlets are transferred directly after formation, without any preceding nonradiative losses such as intersystem crossing (ISC). On the other hand, a triplet state in DCM2 could be excited by close range and possibly slower, triplet-triplet Dexter transfer from the host, as shown in Fig. 1(b). Most fluores-

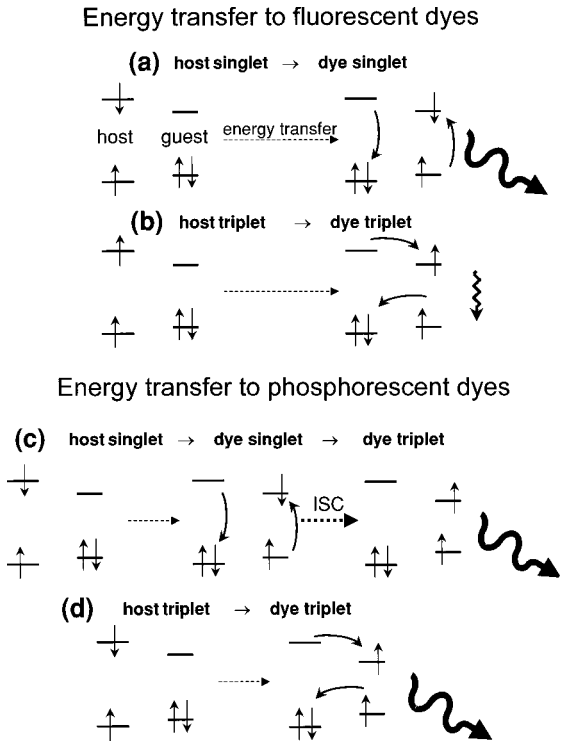

FIG. 1. Proposed energy-transfer mechanisms in films doped with a fluorescent dye (e.g., DCM2:Alq_3) and films doped with a phosphorescent dye (e.g., PtOEP:Alq_3). For each molecule we show the ground-state energy level S_0, the excited-state singlet level S_1 and the excited-state triplet level T_1.

cent dyes (including DCM2) possess short ($\sim$10 ns) radiative lifetimes, and at room temperature, phosphorescence is rarely observed from their triplet states. We assume therefore that all emission from DCM2 ultimately results from singlet states initially formed within the semiconducting host. Figure 1(c) shows singlet-singlet transfer between a host and a phosphor such as PtOEP; it is expected that Förster is still the dominant process in this case. The singlet lifetime of PtOEP is[12] $\lesssim$10 ps and its fluorescence efficiency is[12] 2×10^{-5}. Hence we assume that singlet energy transfer from Alq_3 is followed by ISC in PtOEP with near unity efficiency. Finally, as described previously,[3] Fig. 1(d) represents direct Dexter transfer between triplet states in the host and the phosphor dopant.

To quantify χ_s in an organic host, we write the external EL quantum efficiency (photons extracted in the forward direction per electron injected) as[13,14]

$$\Phi_{\rm el}=[\chi_s\Phi_{\rm fl}\eta_s+\chi_t\Phi_{\rm ph}\eta_t]\eta_r\eta_e. \tag{1}$$

Here, $\chi_t=(1-\chi_s)$ is the triplet fraction of excitons. Also, $\Phi_{\rm fl}$ and $\Phi_{\rm ph}$ are the PL efficiencies of fluorescence and phosphorescence of the acceptor, η_s and η_t are the transfer efficiencies of singlet and triplet excitons from D to A, η_r is the fraction of injected charge carriers that form excitons on the donor, and η_e is the fraction of emitted photons that are coupled out of the device.

By quantitatively comparing the EL efficiencies ($\Phi_{\rm el}^{\rm (fl)}$ and $\Phi_{\rm el}^{\rm (ph)}$) of separate devices employing either a fluorescent or phosphorescent dye, we can use Eq. (1) to determine χ_s and χ_t provided that η_r and η_e are identical in both devices.

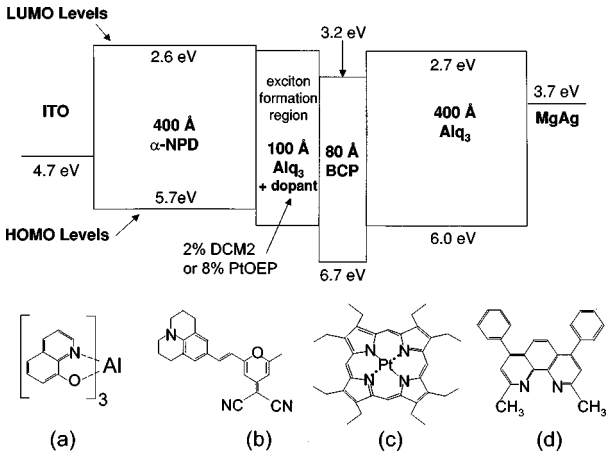

FIG. 2. Proposed energy level diagram of the electroluminescent devices. The luminescent region is sandwiched between electron blocking α-NPD and hole blocking BCP. Three different luminescent regions were employed: undoped Alq_3, which is fluorescent, 2% DCM2 in Alq_3, which is also fluorescent, and 8% PtOEP in Alq_3, which is phosphorescent. Also shown are the chemical structures of (a) Alq_3, (b) DCM2, (c) PtOEP, and (d) BCP.

Furthermore, if all singlets are transferred in both cases (i.e., $\eta_s^{\rm (fl)}=\eta_s^{\rm (ph)}\sim1$), we can obtain χ_s from the ratio of fluorescent and phosphorescent efficiencies ($\Phi_{\rm el}^{\rm (fl)}$ and $\Phi_{\rm el}^{\rm (ph)}$) to obtain

$$\chi_S=\frac{\eta_t^{\rm (ph)}}{\left(\dfrac{\Phi_{\rm el}^{\rm (ph)}}{\Phi_{\rm el}^{\rm (fl)}}\cdot\dfrac{\Phi_{\rm pl}^{\rm (fl)}}{\Phi_{\rm pl}^{\rm (ph)}}\right)-(1-\eta_t^{\rm (ph)})}. \tag{2}$$

Since the ratios reflect relative measurements, the only absolute result required is the triplet state transfer efficiency from the host to the phosphor (i.e., $\eta_t^{\rm (ph)}$).

III. EXPERIMENT

To determine the ratio of the EL efficiency of PtOEP and DCM2 in Alq_3 (i.e., $\Phi_{\rm el}^{\rm (ph)}/\Phi_{\rm el}^{\rm (fl)}$), a series of devices[9] were made using either of these two materials doped into the Alq_3 host (see Fig. 2). Organic layers were deposited in a vacuum of $<10^{-6}$ Torr onto a glass substrate precoated with a 1700-Å-thick layer of indium tin oxide (ITO). A 400-Å-thick film of the hole transport material 4,4′-bis [N-(1-napthyl)-N-phenyl-amino] biphenyl (α-NPD) was deposited on the ITO, followed by a thin (100-Å) doped Alq_3 layer acting as the emissive region. On top of the doped layer, a thin (80-Å) layer of the hole and exciton blocking material[4] 2,9-dimethyl-4,7-diphenyl-1,10-phenanthroline (bathocuproine, or BCP)[15] was deposited. A 400-Å-thick cap layer of Alq_3 was used as buffer between the emissive region and the Mg:Ag (25:1) cathode. Finally, a 1000-Å-thick cap layer of silver was deposited to protect the cathode from decomposition. For comparison, undoped Alq_3 devices were prepared with and without the BCP layer. Samples were mounted directly onto the surface of a calibrated silicon photodetector,[16] and the forward-scattered luminescence was measured.

In Fig. 3 we observe that the efficiency of the Alq_3/BCP device has a slight upward trend but that the efficiency of both doped devices decreases with increasing current; a point

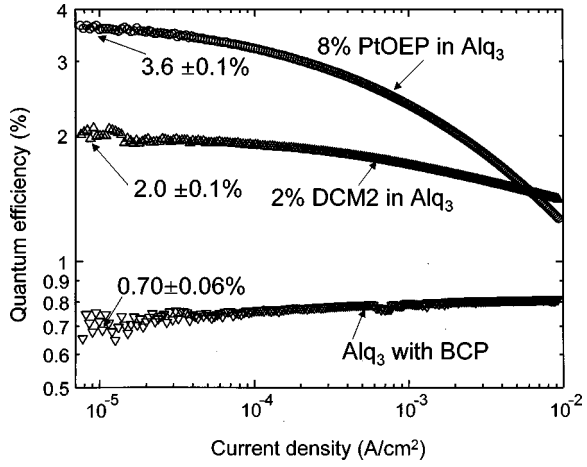

FIG. 3. EL quantum efficiency of the DCM2, PtOEP, and Alq_3-only devices. All curves are constant in the low current regime where multiexciton interactions leading to quenching are negligible. The structure of the devices is shown in Fig. 2. All devices contain a BCP blocking layer.

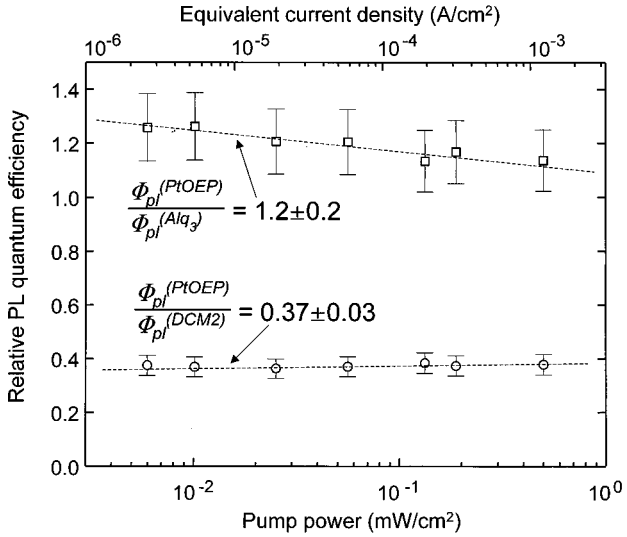

FIG. 4. PL efficiencies of Alq_3 and DCM2:Alq_3 relative to PtOEP:Alq_3. The efficiencies are plotted versus pump power (at 400 nm) and also, for comparison with the EL data, versus an estimation of the current density equivalent to the pump power. The lines are guides to the eye only.

that we will return to in Sec. IV. The efficiency data therefore were obtained at current densities $\lesssim 10^{-5}$ A/cm^2, where both efficiency curves are relatively flat and there is a low density of excited states. In this regime, using the data of Fig. 3, we get $\Phi_{\rm el}^{\rm (DCM2)}/\Phi_{\rm el}^{\rm (PtOEP)} = 0.56 \pm 0.06$ and $\Phi_{\rm el}^{\rm (Alq_3)}/\Phi_{\rm el}^{\rm (PtOEP)} = 0.20 \pm 0.02$.

The values of $\Phi_{\rm pl}^{\rm (PtOEP)}/\Phi_{\rm pl}^{\rm (DCM2)}$, $\Phi_{\rm pl}^{\rm (PtOEP)}/\Phi_{\rm pl}^{\rm (Alq_3)}$, $\eta_s^{\rm (DCM2)}$, and $\eta_s^{\rm (PtOEP)}$ were obtained by optically pumping doped films near the absorption peak of Alq_3 at a wavelength[16] of $\lambda = 400$ nm using a broad-spectrum mercury xenon lamp and monochromator. Photoluminescence from the sample was coupled into a fiber bundle after being filtered to remove interference from the pump and then analyzed using a second spectrometer. As in the case of electrical pumping, low optical pump intensities of $\lesssim 0.2$ mW/cm^2 were used to minimize bimolecular quenching due to dye exciton interactions.[3] Equating the number of photons absorbed with the number of carriers injected in the EL devices and assuming $\eta_r = 1$, yields an equivalent current density of $\sim 10^{-5}$ A/cm^{-2} for these optical pump intensities. The integrated PL efficiency ratios were $\Phi_{\rm pl}^{\rm (PtOEP)}/\Phi_{\rm pl}^{\rm (DCM2)} = (0.37 \pm 0.03)$ and $\Phi_{\rm pl}^{\rm (PtOEP)}/\Phi_{\rm pl}^{\rm (Alq_3)} = (1.2 \pm 0.2)$. The relative PL quantum efficiencies as a function of pump intensity are shown in Fig. 4 and the spectra at a pump power of ~ 10 μW/cm^2 are shown in Fig. 5. The trends in the relative PL data of Fig. 4 match those observed in the EL data of Fig. 3, indicating that similar quenching phenomena occur in both cases. However, the rapid decrease seen, for example in the PtOEP:Alq_3 EL efficiency as the current density increases, is not observed in PL. As discussed in Sec. IV, there are differences between PL and EL processes; and in this work, we attempt to minimize these discrepancies by taking our measurements at very low excitation densities.

No Alq_3 emission was observed in the doped films, hence we conclude that $\eta_s^{\rm (fl)} = \eta_s^{\rm (ph)} = 1$. Note that direct absorption at the pump wavelength of $\lambda = 400$ nm by DCM2 and PtOEP molecules is less than 1% and 8% of the total absorption, respectively.[11,16,17]

To determine $\eta_t^{\rm (ph)}$, we assume that Alq_3 triplets either nonradiatively decay or are transferred to PtOEP. The rate of nonradiative decay is a function of the triplet diffusion length L_d. Similarly, the rate of triplet transfer to PtOEP is proportional to the transfer length L_t, which depends on dopant concentration. For example, low doping densities result in a reduced likelihood of transfer, and we expect this to be reflected in a larger L_t. If A_T^* is the concentration of Alq_3 triplet excited states and x is the distance from the exciton formation zone[7] at the interface between Alq_3 and the α-NPD hole transport layer (i.e., at $x = 0$), then

$$\frac{dA_T^*}{dx} = -\frac{A_T^*}{L_t} - \frac{A_T^*}{L_d} = -\frac{A_T^*}{L}. \tag{3}$$

Since η_t is the ratio of triplets transferred to the total number of Alq_3 triplets formed at the α-NPD interface, then

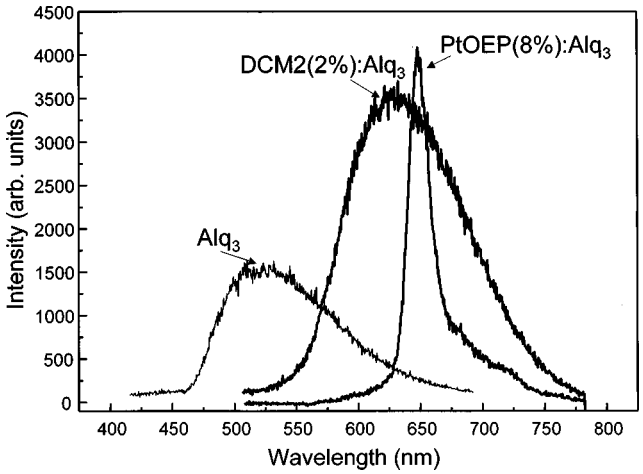

FIG. 5. The PL spectra of Alq_3, DCM2:Alq_3, and PtOEP:Alq_3 at a pump ($\lambda = 400$ nm) intensity of 10 μW/cm^2.

$$\eta_t(d) = \frac{1}{A^*(0)} \int_0^d \frac{A^*(x)}{L_t} dx = \frac{L_d}{L_t + L_d}(1 - e^{-d/L}), \quad (4)$$

where d is the thickness of the doped layer.

To measure L_d, a 100-Å-thick layer of DCM2 doped at 2% molar concentration in Alq_3 was deposited in a vacuum of $<10^{-6}$ Torr onto the surface of a previously deposited α-NPD+copper phthalocyanine hole transport layer on an indium tin oxide (ITO) coated glass substrate [see inset, Fig. 5(a)]. The DCM2 placed in the exciton formation zone of this otherwise conventional[9] organic light emitting device serves to remove singlets through Förster transfer.[3] The diffusion length of the remaining triplet states is determined by depositing an Alq_3 spacer layer between the DCM2 singlet ''filter'' and a 100-Å-thick layer of PtOEP(10%):Alq_3. A second, 300-Å-thick Alq_3 layer located between the cathode and the PtOEP layer reduces exciton quenching at the electrode. As the thickness of the spacer between the singlet filter and the PtOEP is increased, triplets must diffuse farther to reach the PtOEP layer, and its luminescence should decrease accordingly. Within experimental error, however, no appreciable decrease in PtOEP emission was observed even at the maximum spacer thickness of 600 Å. From the data in Fig. 6(a), we estimate therefore that the triplet diffusion length in Alq_3 must be $L_d \geqslant 1400$ Å.

The triplet transfer distance in PtOEP is independently obtained by inserting layers of varying thickness of PtOEP(8%):Alq_3 separated from the DCM2 singlet filter by a 100-Å-thick Alq_3 spacer layer [inset, Fig. 6(b)]. As the thickness of PtOEP increases, the total phosphorescence intensity increases until all Alq_3 triplets are either transferred or else nonradiatively decay. Note that extending the PtOEP layer and, consequently, the proximity of PtOEP sites to the cathode, increases the effect of cathode absorption. However, because most luminescence occurs in the first 100 Å of the PtOEP layer at a distance of over 400 Å from the cathode, cathode quenching effects are small. Figure 5(b) shows the spectral intensity as a function of the phosphorescent layer width. From these data, we obtain $L_t = (140 \pm 30)$ Å and thus $L = (1/L_t + 1/L_d)^{-1} = (125 \pm 25)$ Å. Solving Eq. (4) for the triplet transfer efficiency in a 400-Å-thick PtOEP(8%):Alq_3 layer, we get $\eta_t^{(\mathrm{PtOEP})}(400\,\text{Å}, 8\%) = 0.90 \pm 0.05$.

This result is supported by a comparison of the peak EL quantum efficiency of PtOEP(8%):Alq_3 devices with and without the BCP confinement layer as shown in Fig. 7. The peak efficiencies are 3.6% and 3.2%, respectively, and assuming $\eta_t = 1$ in the device employing BCP (circles), then for the device without BCP (squares) $\eta_t^{(\mathrm{PtOEP})}(400\,\text{Å}, 8\%) = 3.2/3.6 = 0.9$, in agreement with the above calculation. More lightly doped films possess lower transfer efficiencies; for example in Ref. 4 we observed $\eta_t^{(\mathrm{PtOEP})}(400\,\text{Å}, 4\%) \sim 0.7$ (Fig. 7, triangles). The complete energy transfer seen in devices employing the blocking layer supports the hypothesis that the principal action of BCP in Alq_3-based devices is as a barrier to the diffusion of Alq_3 triplet excitons. This finding is also supported by the results in Ref. 5, where phosphorescent efficiencies were observed to increase by an order of magnitude when blocking layers are employed. Hence, we employ BCP in our devices to achieve $\eta_t^{(\mathrm{ph})} \sim 1$.

Given the previous results for the relative EL and PL quantum efficiencies of the devices containing BCP and the calculation of the triplet energy transfer efficiency, we apply Eq. (2) to obtain the spin multiplet fractions of $\chi_s = (21 \pm 3)\%$ for the DCM2/PtOEP system, and $\chi_s = (24 \pm 4)\%$ for the Alq_3/PtOEP system. Here, the error quoted is the quadrature sum of all measurement errors used in the determination of χ_s, which is justified given that the sources of uncertainty in these measurements are uncorrelated. Taking the weighted average of these results, we obtain an overall value for the singlet fraction in Alq_3 of $\chi_s = (22 \pm 3)\%$.

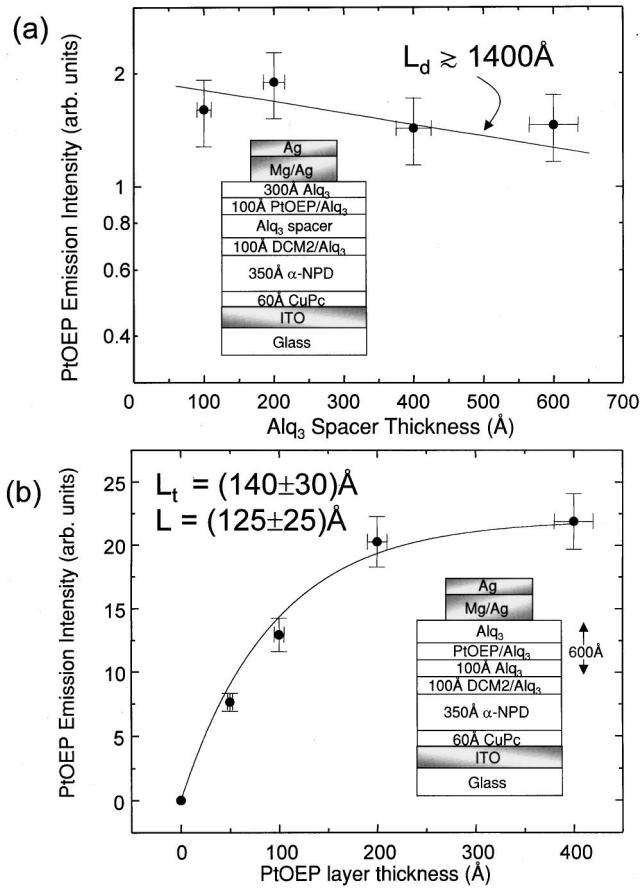

FIG. 6. (a) To determine the triplet diffusion length of Alq_3, we employ the device structure shown in the inset and remove singlet excitons with a 100-Å-thick layer of DCM2(2%):Alq_3. The remaining triplets are forced to diffuse through an Alq_3 spacer layer before reaching a luminescent PtOEP layer. As the thickness of the spacer layer increases, the rate of decrease in PtOEP luminescence gives a triplet diffusion length of $\geqslant$1400 Å. (b) The thickness of the luminescent PtOEP layer is increased until all triplets diffusing through the layer either nonradiatively decay or are transferred to PtOEP. By fitting the measured PtOEP emission intensity to Eq. (6), the combined diffusion and transfer length of triplets in Alq_3 is calculated to be (125±25) Å. From Eq. (5), the transfer length is calculated to be (140±30) Å. The total device thickness was kept constant by adjusting the thickness of the Alq_3 cap layer adjacent to the cathode. Both the transfer and diffusion measurements were made at 6.5 mA/cm^2.

IV. SIGNIFICANCE OF THE RECOMBINATION ZONE

The proposed energy level diagram in Fig. 2 shows that the Alq_3 exciton formation region is surrounded by wide

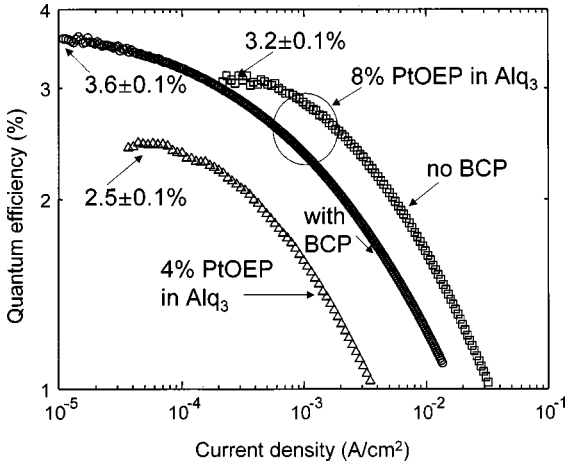

FIG. 7. Electroluminescent (EL) quantum efficiency of PtOEP:Alq_3 devices demonstrating the effect of PtOEP doping density and the BCP exciton blocking layer. The quantum efficiency of a double-heterostructure EL device containing a 100-Å-thick emissive layer of PtOEP(8%):Alq_3 and a 80-Å-thick BCP layer is shown (circles). For comparison, the quantum efficiency of a single heterostructure EL device containing a 400-Å-thick emissive layer of PtOEP(8%):Alq_3 is also plotted (squares). This later device is predicted to have a triplet transfer efficiency of 0.90 ± 0.05. Hence we expect that the double-heterostructure device has a transfer efficiency of ~100%. Also shown (triangles) is the efficiency of a single heterostructure EL device containing a 400-Å-thick emissive layer of PtOEP(4%):Alq_3. The reduction in efficiency may be due to poorer energy transfer in a more diffusely doped device.

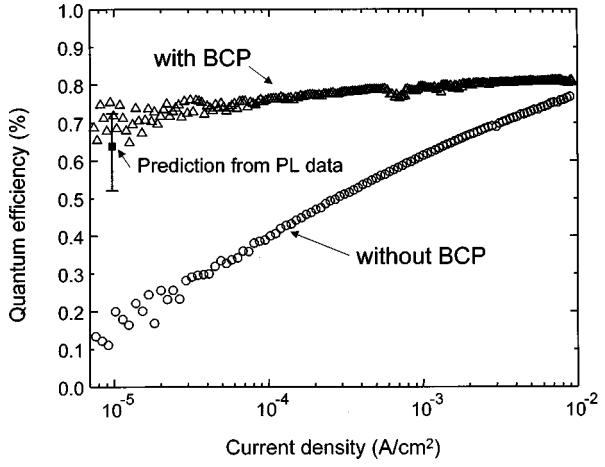

FIG. 8. EL quantum efficiency of the Alq_3-only devices with and without the BCP blocking layer. At $J \sim 10^{-5}$ A/cm^2 the efficiency of the device without BCP is only ~0.2%, which is much less than the expected value of (0.62 ± 0.1)% calculated from the relative PL efficiencies of Alq_3 and DCM2:Alq_3.

energy-gap materials. Thus the presence of the BCP layer creates a double-heterostructure,[18] enforcing identical narrow emission zones in each device, thereby making unbalanced injection unlikely. The disadvantage of employing a heterostructure is that some excitons, notably singlets with their capability for Förster transfer, may be formed in the α-NPD hole transport layer within the energy transfer radius of Alq_3 (~32 Å).[19] However, we consider this possibility to be highly unlikely in our experiments, since even at extremely high injection densities, emission from α-NPD is not observed. Thus the recombination zone, if it exists in α-NPD, must be no wider than a few monolayers.

In principal, it would be preferable to employ single layer Alq_3 devices to eliminate the possibility for recombination outside the desired region. However, the location of the recombination zone is uncertain in single layer structures, and experiments such as those by Cao, *et al.*[20] employing single layer polymer structures do not maintain adequate control over the location of the recombination zone. Hence such measurements must be treated with caution.

The importance of a well-controlled recombination zone is demonstrated by comparing Alq_3-only devices with and without BCP. We find that addition of the BCP blocking layer makes little difference to the doped devices but it significantly reduces the slope of the quantum efficiency of the Alq_3-only devices (see Fig. 8). Furthermore, in the absence of BCP we find that the Alq_3-only devices cannot be compared to the doped devices. For example, from the relative PL data of DCM2:Alq_3 and neat Alq_3 we should be able to predict the EL efficiency of an Alq_3-only device from the EL efficiency of a DCM2:Alq_3 device. Comparing efficiencies at $J \sim 10^{-5}$ A/cm^2, we have $\Phi_{el}^{Alq_3} = \Phi_{el}^{DCM2} \cdot \Phi_{pl}^{Alq_3} / \Phi_{pl}^{DCM2} = (0.62 \pm 0.1)$%. As seen in Fig. 8, the efficiency of the Alq_3-only device without BCP is significantly lower than predicted (solid square) by the relative PL efficiencies. In contrast, there is much better agreement when the emission zone is restricted by a BCP layer. Calculations for Alq_3 heterostructures predict[21] a recombination zone width of ~120 Å. However, the emission zone, as detected by a DCM doped layer,[7] is considerably larger (~400 Å). The difference between the widths of emission and recombination zones is due to exciton diffusion. Hence the discrepancy in efficiency in Fig. 8 is due to the diffusion of Alq_3 excitons to nonradiative sites near the cathode in the absence of a BCP exciton-blocking layer.[4] It is known that doped devices possess a narrow emission zone (~50 Å),[7] with or without a hole blocking layer. Thus relative intensity experiments are justified only when all devices possess emission regions of similar extent.

V. DISCUSSION

Since absolute PL and EL measurements require accounting for every photon[20] and hence are subject to significant systematic error, the technique used here employs relative measurements where possible. For accurate comparisons between different devices, the charge transport layers, injection interfaces and contacts of all devices were fabricated during a single deposition run and hence are identical. In contrast, the measurements of the singlet fraction of excitons in DCM2:Alq_3 and Alq_3-only devices differ fundamentally by the presence of energy transfer in the DCM2:Alq_3 device. For example, the PL efficiency of Alq_3 is 0.32 ± 0.2,[16] giving a nonradiative rate approximately twice the radiative rate ($k_{nr} \sim 2k_r$). Yet, in a DCM2:Alq_3 film, less than 1% of the total emitted photons are observed from Alq_3, therefore, given a DCM2:Alq_3 PL efficiency of ~80%, we infer an energy transfer rate $k_t \sim 50\ k_{nr}$. Hence energy transfer avoids host quenching processes.

Nevertheless, in relative measurements with PtOEP:Alq_3,

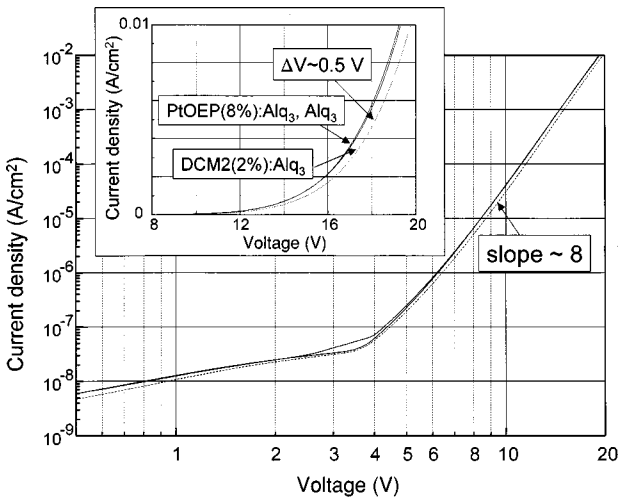

FIG. 9. The current-voltage characteristics of the devices containing BCP. Devices containing PtOEP overlap the characteristic of the Alq_3-only devices, however, DCM2 devices possess a 0.5-V voltage increase, possibly due to trapping on DCM2 molecules.

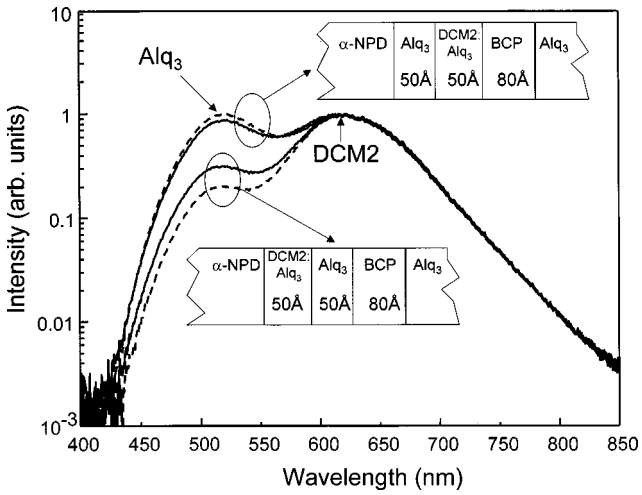

FIG. 10. A demonstration of the effect of BCP on the location of the recombination zone. Dashed lines indicate the spectra of EL devices without a BCP blocking layer. Relative to devices containing BCP, we observe that the bulk of recombination remains at the α-NPD interface, however, BCP is responsible for a compression of the zone and possibly also a slight shift towards the Alq_3/BCP interface. The spectra were recorded at a current density of 60 mA/cm^2. For clarity the spectra have been normalized at the peak of the DCM2 emission (610 nm).

both Alq_3-only and DCM2:Alq_3 systems yield approximately the same value for spin statistics. This is because quenching effects are minimized by measuring *relative* efficiencies at low current densities, with the remaining differences in the nonradiative efficiencies quantified by the PL intensities. For example, intersystem crossing[8] in Alq_3 should not influence the measurement of spin statistics, since it should equally affect both the EL and PL efficiencies. By taking the ratio of the EL and the PL efficiencies as in Eq. (2), the effects of intersystem crossing cancel out.

Thus our measurement of spin statistics cancels the effects of all quenching processes that occur in both EL and PL. However, EL quenching processes which may not be reflected in the PL measurements must also be considered. For example, as shown in Fig. 9, there is a 0.5-V increase in the operating voltage of devices containing DCM2 relative to those containing PtOEP. Analysis of energy transfer has shown that charge trapping and direct exciton formation is not a major effect in PtOEP:Alq_3 films.[3] Thus the discrepancy between the DCM2 and PtOEP device current conduction may imply that a significant fraction of excitons emitted by the DCM2:Alq_3 device originated from trapping of carriers on DCM2, rather than transfer from Alq_3. But previous work has shown[11] that EL in DCM2:Alq_3 is consistent with complete Förster transfer. In addition, we analyzed charge trapping on DCM2 in double heterostructure devices following Tang, VanSlyke, and Tang.[7] That is, the spatial distribution of excitons is probed by moving a DCM2 doped layer within the Alq_3 luminescent layer of the double heterostructure. The EL spectra for different DCM2 layer positions are shown in Fig. 10. The emission from DCM2 ideally should reflect the density of excitons in that region of the undoped double heterostructure. However, if trapping on the dye is significant, the recombination zone should follow the position of the DCM2 layer.[22] In our experiment, we find that significant Alq_3 emission is observed unless the DCM2 layer is positioned immediately adjacent to the α-NPD interface, suggesting that direct charge trapping and exciton formation on DCM2 molecules is probably not significant. This is supported by the equivalence in the singlet fraction obtained from both DCM2:Alq_3 and Alq_3-only devices.

A final point is the influence of the electric field and polaron formation in EL. Measurements[23] of the magnitude of electric-field quenching of Alq_3 luminescence confirm that an external field does indeed lead to exciton dissociation, although the effect is probably not significant at the operating voltages used here. For example, calculations of μE, where μ is the exciton dipole moment and E is the external field, give energies of $\sim$10 meV, much less than the binding energies ($\sim$1 eV) typical of excitons in these materials.

Polaron induced quenching of excitons is also possible, and has been found to have a large effect in some organic materials.[24] However, if polaron quenching were significant in the materials studied here, it is difficult to understand how the Alq_3 quantum efficiency could increase with current. Even with a BCP blocking layer and a restricted recombination zone, there remains a slight upward trend in quantum efficiency. Thus we conclude that quenching due to the electric field or polarons has a negligible effect on the calculation of spin statistics.

VI. CONCLUSION

An accurate determination of exciton spin statistics requires a thorough understanding of exciton formation and energy transfer. Although we cannot definitively rule out quenching due to polarons or direct exciton formation on the dye molecules, this work has presented a consistent set of data yielding a singlet fraction that agrees within error with the expected value of 25%. Both the Alq_3/PtOEP:Alq_3 and the DCM2:Alq_3/PtOEP:Alq_3 systems yield similar results indicating that direct exciton formation on DCM2 molecules is probably not significant. While further work is required to-

understand exciton formation in doped materials, the techniques presented in this work offer an precise method for the determination of spin statistics. Indeed, it should be possible to extend the techniques introduced in this study to different hosts and different temperatures.

ACKNOWLEDGMENTS

This work was funded by NSF and AFOSR. The authors gratefully acknowledge informative discussions with Dr. Paul Burrows, Dr. Vladimir Bulović, and Dr. Scott Sibley.

*Present address: Department of Physics, Trinity College Dublin, Dublin 2, Ireland.

[1] A. R. Brown, K. Pichler, N. C. Greenham, D. D. C. Bradley, R. H. Friend, and A. B. Holmes, Chem. Phys. Lett. **210**, 61 (1993).
[2] S. R. Forrest, Chem. Rev. **97**, 1793 (1997).
[3] M. A. Baldo, D. F. O'Brien, Y. You, A. Shoustikov, S. Sibley, M. E. Thompson, and S. R. Forrest, Nature (London) **395**, 151 (1998).
[4] D. F. O'Brien, M. A. Baldo, M. E. Thompson, and S. R. Forrest, Appl. Phys. Lett. **74**, 442 (1999).
[5] M. A. Baldo, S. Lamansky, P. E. Burrows, M. E. Thompson, and S. R. Forrest, Appl. Phys. Lett. **75**, 4 (1999).
[6] V. Cleave, G. Yahioglu, P. Le Barny, R. Friend, and N. Tessler, Adv. Mater. **11**, 285 (1999).
[7] C. W. Tang, S. A. VanSlyke, and C. H. Chen, J. Appl. Phys. **65**, 3610 (1989).
[8] R. Ballardini, G. Varani, M. T. Indelli, and F. Scandola, Inorg. Chem. **25**, 3858 (1986).
[9] S. A. VanSlyke and C. W. Tang, U.S. Patent No. 4539507 (1985).
[10] M. Klessinger and J. Michl, *Excited States and Photochemistry of Organic Molecules* (VCH Publishers, New York, 1995).
[11] V. Bulovic, A. Shoustikov, M. A. Baldo, E. Bose, V. G. Kozlov, M. E. Thompson, and S. R. Forrest, Chem. Phys. Lett. **287**, 455 (1998).
[12] G. Ponterini, N. Serpone, M. A. Bergkamp, and T. L. Netzel, J. Am. Chem. Soc. **105**, 4639 (1983).
[13] T. Tsutsui and S. Saito, in *Intrinsically Conducting Polymers: An Emerging Technology*, edited by M. Aldissi (Kluwer Academic, Dordrecht, 1993), Vol. 246, p. 123.
[14] L. J. Rothberg and A. J. Lovinger, J. Mater. Res. **11**, 3174 (1996).
[15] Y. Kijima, Spring Meeting of the Materials Research Society, San Francisco, 1999, Paper G2.1 (in press).
[16] D. Z. Garbuzov, V. Bulovic, P. E. Burrows, and S. R. Forrest, Chem. Phys. Lett. **249**, 433 (1996).
[17] S.-K. Lee and I. Okura, Anal. Chim. Acta **342**, 181 (1997).
[18] C. Adachi, T. Tsutsui, and S. Saito, Appl. Phys. Lett. **57**, 531 (1990).
[19] R. Deshpande, V. Bulovic, and S. Forrest, Appl. Phys. Lett. **75**, 888 (1999).
[20] Y. Cao, I. Parker, G. Yu, Z. Gang, and A. Heeger, Nature (London) **397**, 414 (1999).
[21] J. Kalinowski, N. Camaioni, P. Di Marco, V. Fattori, and A. Martelli, Appl. Phys. Lett. **72**, 513 (1998).
[22] J. Yang and J. Shen, J. Appl. Phys. **84**, 2105 (1998).
[23] W. Stampor, J. Kalinowski, P. D. Marco, and V. Fattori, Appl. Phys. Lett. **70**, 1935 (1997).
[24] H. Hieda, K. Tanaka, K. Naito, and N. Gemma, Thin Solid Films **331**, 152 (1998).